

## Steady-State Operation with Transport Barriers and Control by On/Off-Axis Current Drive on ASDEX Upgrade

GRUBER Otto\*, WOLF Robert, BOSCH Hans-Stephan, DUX Ralf, GUENTER Sybille, McCARTHY Patrick<sup>1</sup>, LACKNER Karl, MARASCHEK Marc, MEISTER Hans, PEREVERZEV Grigori, STAEBLER Albrecht, TREUTTERER Wolfgang and the ASDEX Upgrade Team

*Max-Planck-Institut für Plasmaphysik, EURATOM Association, D-85748 Garching*

<sup>1</sup>*University College Cork, Association EURATOM-DCU, Cork, Ireland*

(Received: 22 February 2000 / Accepted: 13 July 2000)

### Abstract

This paper reviews the scenarios and physics of advanced tokamak discharges and the associated technical enhancements leading towards enhanced performance and steady-state operation in ASDEX Upgrade.

A stationary advanced tokamak scenario with internal transport barriers (ITB) in combination with an H-mode barrier and weak shear ( $q_{min} \approx 1$ ) was maintained for 40 confinement times and several internal skin times with  $H_{ITERL-89P} \beta_N \approx 5$ . By raising the triangularity of the plasma shape the performance was increased up to  $H_{ITERL-89P} \beta_N \approx 7.2$ , but  $\beta$  is still limited by neoclassical tearing modes. The density was raised to close to 50% of the Greenwald density either by edge gas fuelling, causing an increase of the threshold power to sustain an ITB and a decrease of  $Z_{eff}$  below 2, or by improved core particle confinement with more triangular plasma shapes without changing the ITB onset conditions. Sufficient He pumping and no temporal impurity accumulation was observed despite peaked impurity density profiles.

MHD modes contribute to making the shear profile stationary. In the ITB/H-mode scenario (1,1) fishbones clamp the q-value in the vicinity of one and avoid sawteeth, while in ITB scenarios with reversed shear ( $q_{min} \approx 2$ ) (2,1) fishbones can clamp the current profile development near the  $q = 2$  surface without deteriorating energy confinement. Double-tearing modes act similarly, but lead to substantial confinement losses.

Applying central ECRF heating and current drive to beam heated reversed shear ITB discharges shows a substantial effect on MHD stability, affecting the passage of the q-profile through  $q_{min} = 2$  and degrading or prolonging the reversed shear phase, depending on the CD direction. Moreover, reactor-relevant  $T_e \geq T_i$  operation with temperatures in excess of 10 keV was achieved with internal transport barriers for both electrons and ions simultaneously.

For current profile control ECCD will be supplemented by on-axis fast wave ICCD and off-axis current drive up to 400 kA using NBI (available in 2001) and ICRF mode conversion. Stationary discharges with RS and  $q_{min} > 2$  should then be possible at a plasma current of 1 MA according to power deposition, current drive, and transport calculations.

\*Corresponding author's e-mail: oxg@ipp.mpg.de

## 1. Introduction

While the ITER design provides for the first time an integral solution for a burning fusion plasma machine, the efforts for conceptual improvements are mainly concentrated on the issues of stationary operation and further optimization with advanced scenarios towards smaller machines. The aspect of steady-state tokamak operation is twofold. First, stationary tokamak operation requires maintenance of the plasma current, for which purpose methods have to be developed to provide a high fraction of internal diffusion driven 'bootstrap' current supplemented by external inductively and non-inductively driven currents. Partial use of the inductively driven currents limit tokamak operation to a stationary, but still pulsed system, while an available combination of bootstrap and external non-inductive current drive offers the route towards steady-state operation. Recent experiments as well as theory show clear indications that appropriate control of the current profile can lead to further confinement improvements resulting in internal transport barriers (ITB) whose pressure gradients can drive the required bootstrap currents [1-4]. This positive feedback loop affords hope of obtaining a fusion reactor significantly smaller in size.

The second main item of stationary tokamak operation is to achieve compatibility of this new concept with sufficient heat and particle exhaust and adequate impurity control and helium ash removal. This has to be realized in conjunction with a sufficient lifetime of the first wall and divertor components and needs an integral solution with sufficient high edge densities, heat load distribution via impurity radiation, impurity screening, helium ash removal, and high heat flux resistant materials.

On ASDEX Upgrade, various scenarios of advanced tokamak concepts have been investigated to achieve improved core confinement by modifying the current density profile by means of early heating in the current ramp to reduce current diffusion at low initial densities. The two scenarios described below were found to be most promising for stationary operation and enhanced performance.

1) ITBs in combination with an H-mode edge barrier and a flat q-profile with  $q_{min} \geq 1$  and  $s \approx 0$  offer stationary, inductively driven H-mode operation with enhanced performance in respect of confinement and  $\beta$  (see Sec. 2 and 3) [5-7]. Access to ignition even in the ITER FEAT may be feasible. With these weak shear profiles  $\beta_N$  is limited by (3,2)-neoclassical tearing modes

depending on the triangularity of the plasma shape.

2) ITBs with flat or reversed shear (RS) and  $q_{min}$  values above 1.5, which exhibit, at least in combination with an L-mode edge, steep pressure gradients in the barrier region and therefore bootstrap currents above 50% of the plasma current [6,7]. Until recently, this scenario was only transiently established during the current ramp-up in ASDEX Upgrade in a limiter configuration. It offers the route to true steady-state, non-inductively driven tokamak operation combining improved performance and high bootstrap current fraction  $f_{bs} = I_{bs}/I_p \propto \beta_N q_{95} \sqrt{A}$ , at high  $q_{95} \geq 4$  and  $\beta_N > 4$ . Low (m,n) neoclassical tearing modes are avoided by the reversed shear and  $q_{min} > 2$ , but double tearing, infernal and external kink modes tend to be unstable [9] and need additional measures for stabilization (see Sec. 5).

This paper reviews the results from the two years of advanced tokamak operation on ASDEX Upgrade, highlights latest results showing progress on unresolved issues towards stationary and reactor-relevant operation, e.g. operation at higher performance and densities with  $Z_{eff} < 2$ , reactor-relevant  $T_e \geq T_i$  operation with central counter-ECCD in RS discharges, and describes the technical enhancements for steady-state operation.

## 2. Steady-State ITB Discharges Combined with H-mode Edge Barrier at Low Central Shear ( $q_{min} \approx 1$ )

A stationary regime of operation has been found which shows improved core confinement of both electrons and ions caused by an internal transport barrier in combination with an H-mode edge [5-7]. In Fig. 1, the main plasma parameters of such a discharge are illustrated. During the current ramp moderate neutral beam heating of 2.5 MW is applied, while in the current flat-top after  $t = 1$  s the NBI power is raised to 5 MW and the line-averaged density is kept at  $4 \times 10^{19} \text{ m}^{-3}$  (low compared with Greenwald density,  $\approx 0.3 n_{GW}$ ). Just before 1 s the X-point is formed and the internal barrier formation and the L-H-transition occur within 20 ms.

While the electron and ion temperatures increase at the same rate during the current ramp at a heating power of 2.5 MW,  $T_i$  (from CXRS) reaches almost twice the value of  $T_e$  (from ECE and Thomson scattering) when the heating power is doubled since 75% of the heating power goes to the ions. Central values of  $T_i = 10$  keV and  $T_e = 6.5$  keV,  $H_{ITERL-89P} = 2.4$  or  $H_{ITERH-92P} = 1.4$  and  $\beta_N = 2$  at  $q_{95} = 4.5$  are maintained for 6 s, limited only by the duration of the pulse length. This corresponds to 40 confinement times and 2.5 resistive time scales for

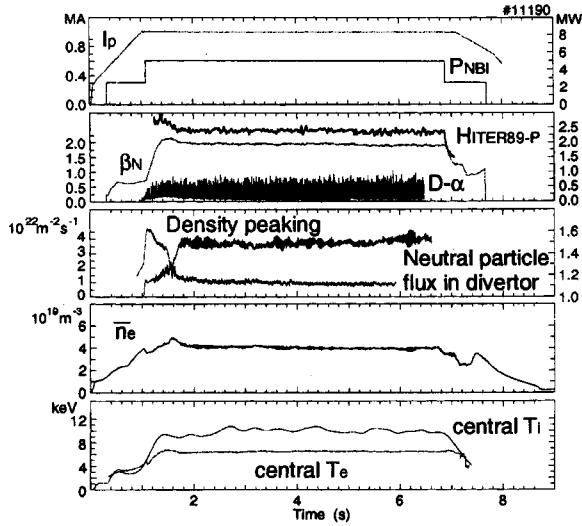


Fig. 1 Time evolution for a steady-state discharge with ITB and H-mode edge ( $B_t = 2.5$  T).

internal current redistribution. Even the current profile remains stationary shortly after the creation of the barriers as measured by a 10-channel motional Stark effect (MSE) polarimeter in combination with equilibrium reconstruction from magnetics (CLISTE code). In addition, the measured loop voltage is also stationary within 10%. Raising the triangularity of the plasma shape increased performance up to  $H_{ITERL-89P} \beta_N \approx 7.2$  (at  $q_{95} = 5.5$  with  $H_{ITERL-89P} = 3$ , see Sec. 4), but  $\beta$  is still limited by neoclassical tearing modes ( $\beta_{N,onset} \approx 2.6$ ).

The profiles of the plasma temperatures, density, and toroidal rotation velocity show, in addition to the H-mode edge pedestal, an increase starting at  $\rho_{tor} = 0.6$ . Thereby, the central  $T_i$  and the toroidal velocities are about a factor of two above the conventional sawtoothed ELMy H-mode level (at the same discharge parameters). These differences are also reflected in the lower performance parameters of the conventional H-mode discharge with  $H_{ITERL-89P} = 1.8$  and  $\beta_N = 1.6$ .

Energy transport was analyzed with the 1-1/2-D ASTRA code. In the central regions of the plasma the ion thermal conductivity drops to neoclassical values, but the electron thermal conductivity is also at a low level, indicating that transport reduction is not limited to the ions. ASTRA transport simulations reveal that, in addition to magnetic shear stabilization, a combination with  $E \times B$  velocity shear stabilization is required to explain the observed reduction of thermal transport  $\chi$  coefficients [10]. The  $E \times B$  shearing rate is above the

linear turbulence growth rates for  $\rho_{tor} < 0.5$ , and even for  $\rho_{tor} > 0.5$  a strong reduction of  $\chi$  is calculated as a result of shear stabilization. Best agreement with the measured profiles was found with the Weiland-Nordmann ITG model, where the measured radial electric field was taken into account.

In the combined ITB and H-edge barrier scenario discussed here, the only MHD activities observed in the core of the plasma are strong (1,1) fishbones which start at 1.1 s and accompany the entire 5 MW heating phase. These fishbone oscillations are driven by passing fast particles and behave like a resistive MHD instability similar to sawteeth, but on a much faster time scale of 1 ms. This drives a magnetic reconnection process and causes stationary clamping of the core q-profile even in the absence of sawteeth in agreement with the measured q-profile showing an extended central low-shear region (magnetic shear  $s = r dq/dr/q \approx 0$  within  $\rho \approx 0.35$ ) with  $q_o \approx 1$  [5,7,8]. These fishbones also affect transport, but only to a small extent. Reduced impurity peaking (from central SXR radiation), but nearly no decrease of core electron temperatures (from ECE) are observed comparing phases with and without fishbones, where the last ones can last up to 50 ms. No direct diagnostic for fast ions losses was available.

The calculated current density profiles from ASTRA give a bootstrap current maximum close to the centre due to the limited pressure gradient and a total of 25% of the plasma current corresponding to the moderate  $\beta_N$  values (65% ohmic, 10% NBI current drive).

### 3. High-density Operation, Threshold Power for ITB Formation and Influence of Plasma Shape

An integrated stationary scenario needs sufficiently high densities at the plasma edge and separatrix to provide divertor operation with sufficient power exhaust. Secondly, high-density operation is required to establish sufficiently high core densities for fusion power production.

Raising the density by gas fuelling at constant heating power resulted in deterioration of confinement in these H-mode edge scenarios [5]. In the last campaign the density has been extended to slightly below half of the Greenwald density by applying a simultaneous power ramp [7]. In Fig. 2 such a discharge is shown where the line-averaged density has been increased from  $3.5 \times 10^{19} \text{ m}^{-3}$  to  $5.5 \times 10^{19} \text{ m}^{-3}$ . Clearly the threshold for heating power (or torque input) to sustain the ITB is

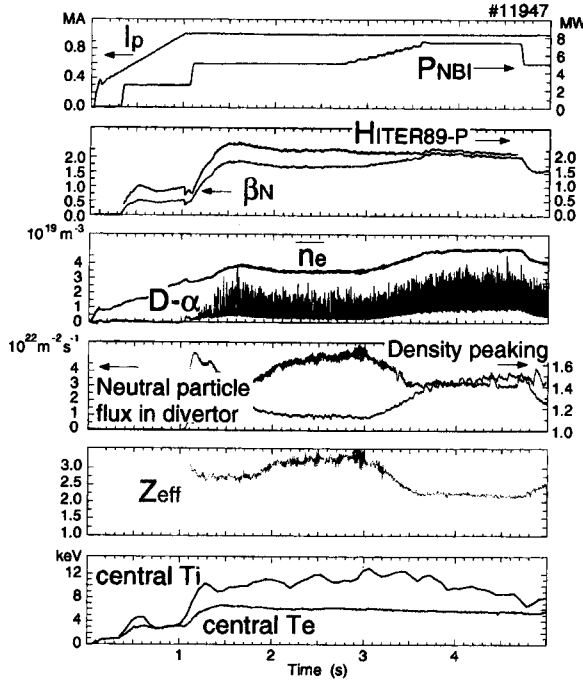


Fig. 2 Time evolution of a double barrier discharge with density ramp by gas fuelling ( $B_t = 2.5$  T).

increased with rising density by means of external gas puffing (by about 50% in the case shown). There was no confinement deterioration and therefore  $\beta_N$  increased, while the density peaking decreased only moderately. Obviously, the core  $Z_{eff}$  decreased from 3 to 2 for the higher density case due to the increased impurity screening at higher SOL densities. Further density rise was again limited by neoclassical tearing modes caused by  $\beta$  rising up to the stability limit at  $\beta_N = 2.2$  with increasing heating power (all experiments were done at  $\langle \delta \rangle = 0.2$ ).

The density could also be raised by using plasma shapes with higher triangularity in an attempt to increase the stability limit of neoclassical tearing modes [7]. Plasma shapes with higher triangularities can be run in the present ASDEX Upgrade divertor IIa with the outer strike point on the roof baffle after modification of the ICRH antennae. During a slow increase of  $\langle \delta \rangle$  from 0.2 to 0.3 (the upper triangularity is predominantly changed) and a slightly enhanced heating power (5 MW  $\rightarrow$  6.25 MW) the plasma energy increases by almost 30% to  $\beta_N = 2.4$  (at  $H_{ITERL-89P} = 3.0$ ) without excitation of NTM's. The observed plasma energy increase and confinement improvement are mainly due to a density rise up to 0.45  $n_{GW}$  and have to be mainly attributed to the higher H-mode pedestal pressure at the higher triangularity

leading to improved edge MHD stability. This density increase at higher triangularities occurs without gas fuelling and therefore at a low neutral particle flux outside the SOL in contrast to the density ramp scenario described before, where the density increase was driven by external gas fuelling and consequently high neutral particle fluxes. The triangularity obviously improves the core particle confinement, while the core energy confinement increases only slightly. This is in contrast to conventional H-mode discharges, where edge and core energy confinement are related by stiff temperature profiles and both increase with triangularity [11].

A major concern regarding stationary plasma operation with improved core confinement is the impurity transport, since high impurity content or  $Z_{eff}$  leads to dilution of hydrogen ions and may cause high radiation losses. The time evolution of the SXR emission indicates no temporal accumulation of impurities from 2 s until the end of the 5 MW heating phase of the discharge shown in Fig. 1. With the presence of elements with  $Z$  larger than Si being neglected, an upper limit of  $Z_{eff} \approx 3$  is derived [12]. The impurity content and  $Z_{eff}$  profiles are slightly peaked in the plasma centre, and quasi-stationary after 2 s. But nevertheless the deuteron density still increases towards the plasma centre. The stationarity is possibly caused both by the strong fishbone activity expelling impurities from the plasma core, such as sawteeth, and by the ELM activity at the edge. The behaviour of medium- $Z$  impurities was investigated by Ar puffing. Analyses revealed peaked impurity density profiles which are within the uncertainties consistent with neoclassical predictions. Despite the increasing convective inward transport due to the strong density peaking the temperature screening is strong enough to keep the high- $Z$  densities stationary.

Helium transport and exhaust were investigated by means of short, external gas puffs in the midplane. The resulting helium profiles measured with CXRS do not reveal any sign of radial transport into the core and helium exhaust is still determined by transport in the scrape-off layer and divertor region. The exhaust rate increases with the divertor neutral flux density [13] and is faster than expected from conventional ELMy H-mode discharges.

#### 4. ITB Discharges with Reversed Shear and $q_{min} > 1.5$

Reversed shear scenarios with internal barriers were established during the current ramp phase by

applying 5 MW NBI, resulting in strongly reversed shear (see Fig. 3) [6,8]. These discharges have an L-mode edge due to an enforced limiter configuration or a single null divertor configuration with the ion- $\nabla B$  drift away from the X-point. Steep pressure gradients with central values of  $T_i = 15$  keV and  $T_e = 5$  keV were obtained with NBI heating, but due to both the smaller radius of the barrier and the L-mode edge the plasma performance is reduced with a confinement enhancement factor  $H_{ITERL-89P} = 1.9$  and  $\beta_N = 1.6$ . The bootstrap current amounts to 55% and is peaked at the pressure barrier position (35% ohmic, 10% NB current drive). In the barrier region both electron and ion thermal conductivities are close to the ion neoclassical values, while the transport coefficients strongly increase towards the L-mode plasma edge [6]. Good agreement is again obtained with ASTRA transport simulations using the Weiland-Nordmann ITG model [10]. Recently, the SN discharges could be extended into the flat-top phase for some confinement times, with a barrier position shifted to a larger radius  $\rho \approx 0.5$  at 7.5 MW heating power. When  $q_{min}$  falls below two, (2,1) MHD modes destroy the performance of these discharges and, depending on the edge q-value, may also lead to disruptive termination.

Strong MHD activity is observed in this scenario. Low (m,n) neoclassical tearing modes are avoided by the reversed shear and  $q_{min} > 2$ , while the temperatures outside the barrier towards the plasma edge are low enough to avoid (5,2) modes. But in the evolution of the very hollow q-profile (measured by MSE) due to the constantly penetrating current - the edge q is still decreasing during the current rise - many resonant q surfaces for MHD modes are passed. These modes can cause severe energy losses, but might help to achieve quasi-stationary advanced discharges by clamping of the q-profile [8]. Short stationary phases are obtained with  $q_{min}$  fixed at 3 and finally 2 for up to 200 ms (see fig. 3 between 0.6 and 0.7 s). When  $q_{min}$  reaches two, (2,1) fishbones are often observed which clamp the current profile by magnetic reconnection without global confinement losses, like the (1,1) fishbones in the double-barrier discharges described in Sec. 2. However, the also existing (2,1) continuous double-tearing modes - which can also clamp the q-profile - deteriorate confinement (see temperature and  $n = 1$  MHD signal in Fig. 3) and can at least transiently destroy the ITB. Analysis with a nonlinear MHD code shows flattening of the q-profile around  $q_{min} = 2$  by current diffusion and can explain the observed stationarity in time. These

modes are finally stabilized again when  $q_{min}$  falls below 2, so that the differential rotation and the increasing distance between the rational  $q = 2$  surfaces become large enough to decouple the resonant surfaces [8].

## 5. Response of ITB with RS to Central ECRH and ECCD

Clamping of the q-profile by reconnecting MHD modes seems to offer a tool to facilitate and control establishment of advanced scenarios. But stationary sustainment of reversed-shear scenarios requires external on-axis or off-axis driven currents. Central current drive by ECRF waves is an effective means of controlling the core shear behaviour, since high electron temperatures and the low fraction of trapped particles improve CD efficiency. Moreover, electron cyclotron heating affords help in demonstrating reactor-relevant  $T_e \geq T_i$  operation. Experimental access to this regime is hampered by the fact that electron heating by neutral beams is reduced in this regime, making combined NBI and ECRH the method of choice for its exploration.

These possibilities have been exploited on ASDEX Upgrade by using 1.2 MW of coupled ECRF power with steerable mirrors [14]. In reversed-shear discharges with L-mode edge ECRF (pure heating or counter-CD mode) was found to facilitate stable passage through the  $q_{min} = 2$  stage by avoiding disruptive double-tearing modes and to prolong the reversed-shear phase.

Although the NBI heating power in these discharges is typically a factor of  $\sim 4$  higher than the

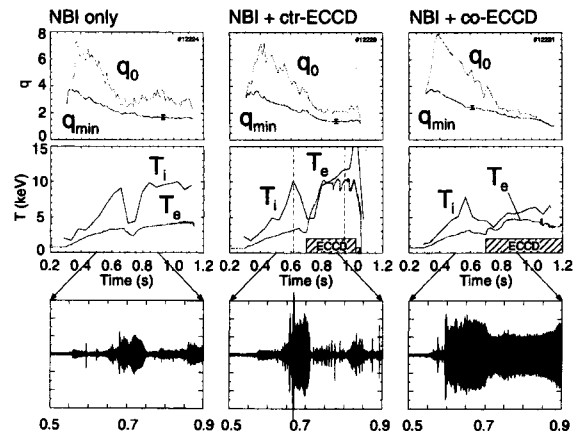


Fig. 3 Comparison of heating scenarios during current ramp: a) reference case with NBI only; b) NBI and counter-ECCD, c) NBI and co-ECCD (time traces of  $q_0$ ,  $q_{min}$ , central  $T_i$  and  $T_e$  values, and MHD Mirnov signals for  $n = 1$  modes;  $I_p = 1$  MA,  $B_i = 2.45$  T).

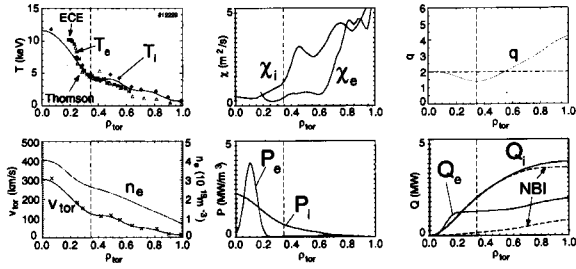


Fig. 4 Profiles of ion and electron  $T$ , density, toroidal rotation velocity,  $q$ , power deposition profiles  $p$  and the corresponding heat fluxes  $Q$  and the resulting heat diffusivities of the discharge shown in Fig. 3b at 0.95 s ( $I_p = 1$  MA,  $B_t = 2.45$  T).

ECRH, in the central region inside the ITB ( $\rho_{tor} \approx 0.3$ ) the deposited ECRH and NBI powers are almost equal (see Fig. 4). This central electron heating and the reduced electron thermal conductivity result in  $T_e \approx T_i$  in the case of pure EC heating and especially with EC counter-CD. Figure 3 compares the time traces of the central  $T_i$  and  $T_e$  (from ECE at  $\rho_{tor} = 0.2$ ) for three heating scenarios: NBI alone, NBI with ctr-ECCD and with co-ECCD. The large drop of  $T_i$  and  $T_e$  before ECRH is switched on is caused by the (2,1) DTM as described above, which is destabilized only transiently and disappears after  $q_{min}$  has passed two (see  $n = 1$  MHD signal). In the ctr-ECCD scenario the electron temperature of 10 keV even 0.12 m from the centre is also confirmed by Thomson scattering.

Both the ion and electron temperatures show an ITB just inside the  $q_{min}$  radius (Fig. 4). The heat conductivities show  $\chi_e \approx \chi_i < 0.5$   $m^2/s$ , where  $\chi_i$  is close to the ion neoclassical value. Despite the fivefold increase of the central electron heat flux to 1.3 MW inside  $\rho = 0.3$  (mainly from ECRH, but including all electron heat sources) the electron heat diffusivity did not increase in relation to NB heating alone. This is besides the high  $\nabla T_e$  a clear indication for an electron transport barrier.

Moreover,  $T_i$  and toroidal rotation did not decrease with respect to the case of pure NBI heating [14]. With co-ECCD the faster decaying central  $q$ -profile leads to enhanced MHD activity of the (2,1) mode (seen also by the modulation of the central  $T_e$  amplitude), and the confinement does not recover after  $q_{min}$  has dropped below 2, since the (2,1) mode persists due to the accelerated decay of the reversed-shear configuration.

## 6. Extensions for Steady-state Non-inductive On/Off-axis CD Scenarios and Current Profile and MHD Control

Study of advanced tokamak scenarios is considered to be a major issue of the ASDEX Upgrade programme. The device has a high plasma-shaping capability up to triangularities of  $\delta = 0.5$  at the separatrix, flexible heating (nearly perpendicular NBI / 20 MW, ICRH / 6 MW, ECRH / 2 MW), refuelling (main chamber and divertor gas-puffing, high and low field-side pellet injectors with velocities of up to 1000 m/s), and elaborate digital control systems. But stationary sustainment of reversed- or low-shear scenarios against the tendency of the inductively driven current to peak centrally at the highest electron temperatures and control of the shear profile (e.g. alignment with the transport barrier) require externally driven currents.

To establish the CD level and its radial distribution for achieving stationary optimal shear profiles, two sets of transport simulations were performed with the ASTRA code. In the first set, temperature and density profiles with an ITB at about half the plasma radius are imposed and just the current diffusion was simulated. For a bootstrap current fraction of 70 % and  $T_e(0) = 10$  keV fully non-inductively driven quasi-stationary reversed-shear operation with  $q_{min} \geq 1.5$  requires an off-axis co-CD peaked at  $\rho \approx 0.5$  with a rather broad profile (e.g. provided by NBCD, see below). These results are rather insensitive to the plasma parameters provided the pressure gradient is sufficiently high.

In the second set the full transport equations are solved self-consistently and the heating and CD time scenarios are optimized to achieve and maintain shear-optimized profiles aligned with the pressure transport barrier [15]. To create the ITB, the thermal conductivities for both ions and electrons are reduced to the ion neoclassical value inside the reversed/weak shear region with  $dq/dr \leq 0$ . The results of the current diffusion simulations described above were confirmed and extended. For instance, reversed shear operation with  $q_{min} \geq 1.5$  is also possible with on-axis ctr-CD of about 150 kA at  $I_p = 1$  MA (already possible with 1.6 MW coupled ECRF according to TORAY calculations). To achieve a well-pronounced stationary reversed shear configuration with  $q_{min} > 2$  at  $\rho \approx 0.6$ , driven currents of about 150 kA are needed in addition to the off-axis NBCD of 250 kA. This current also has to be driven off-axis at  $\rho \approx 0.6$  and could be provided by ICCD (6 MW using mode conversion is available in 2000) or ECCD (1.6 MW injection at the high field side).

These results provide the basis for the CD extensions now being implemented on ASDEX Upgrade for current profile control, stabilization of neoclassical modes, non-inductive on-axis seed currents (to limit  $q_0$ ), and stationary shear configurations. The basis for the off-axis CD will be provided by the 100 keV NB injector, requiring more tangential injection. But turning of the injector box is limited to a tangency radius of 1.29 m, compared with  $R_0 + a/2 = 1.9$  m, due to space restrictions around the device and the port geometry. Off-axis beam deposition can therefore only be achieved by modifying the geometry of two beams (out of four) in the beam line to inject above/below the plasma centre, i.e. by further inclining the beams with respect to horizontal and/or shifting the vertical cross-over point of the two beams further away from the plasma (see Fig. 5) [16].

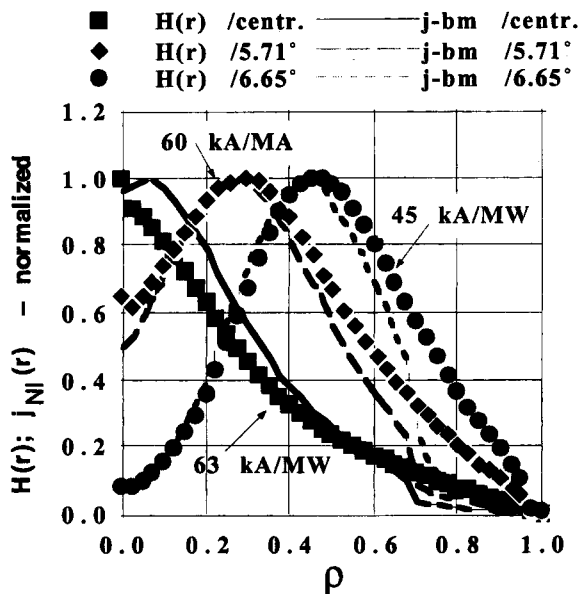
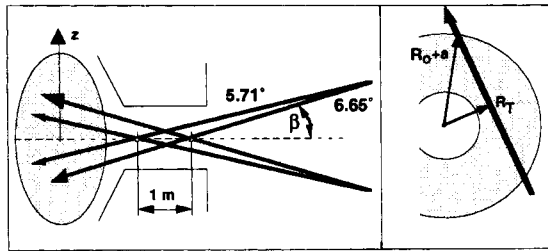


Fig. 5 Sketch of geometry for one pair of beams and NBI deposition profiles compared to NB current drive profiles for three injector geometries with  $R_T = 1.29$  m ( $n_e = 4 \times 10^{19} \text{ m}^{-3}$ ,  $T_e(0) = 4 \text{ keV}$ ).

Keeping  $R_T = 1.29$  m fixed, off-axis deposition peaked around  $\rho \approx 0.5$  is achieved for an inclination angle of 6.7° (presently 4.9°) and for an outward shift of the cross-over point of 1 m. Figure 5 also shows that the beam particle deposition profiles and the current drive profiles are closely related except for the plasma edge, where trapped orbit effects and fast particle losses are to be expected. These deposition profiles are fairly independent of plasma and beam parameters. Changing the beam penetration by a factor of 2.5 by varying the line-averaged density and/or the beam energy does not change the position of the off-axis maximum. This also holds for different density profile shapes and vertical shifts of the plasma position within 0.15 m due to superposition of the top and bottom beams. The total driven current changes according to the expected  $T_e$  and  $n_e$  dependence and for temperatures below 3 keV outside the ITB region is only marginally increased when going to higher beam energies (this effect is enhanced by taking the shinethrough into account). The two other beams of the injector remain unchanged and are therefore still available for central heating.

Current profile control requires real-time information on the current profile to act with the predefined non-inductive CD systems according to the control parameters ( $q_0$ ,  $q_{min}$ ,  $I_p$ ). The standard method for real-time plasma equilibrium parameter identification from magnetic measurements on ASDEX Upgrade is function parametrization (FP). A FP version is now being prepared which will also process the combination of external magnetic measurements and current profile information provided by our 10-channel MSE diagnostic or by MHD mode signals (e.g. SXR). Here, the training database of simulated equilibria with the predictive Garching Equilibrium Code uses a specific parametrization of the equilibrium pressure and poloidal current source profiles, which are then constrained by the current profile information.

In the reversed-shear discharges described in Sec. 4 the fast  $T_e$  crashes were attributed to pressure driven ideal modes in the presence of small shear (infernal modes). The coupling of these modes to excited external kink modes when  $q$  at the edge passes rational values may be the cause of the disruptive termination of the discharge [9]. These low- $n$  free boundary kink modes also limit the  $\beta$ -values attainable for optimized pressure and magnetic shear profiles. We are now investigating the introduction of stabilizing conductive structures on the low field side, designed to suppress these instabilities and to complement them by an active

feedback system using saddle coils capable of acting on the resistive wall time.

## 7. Summary

On ASDEX Upgrade progress towards stationary advanced tokamak operation has been achieved in ITB discharges with both flat shear with  $q_{min} \approx 1$  and reversed shear with  $q_{min} > 2$ . Stationary discharges with an ITB in combination with an H-mode edge barrier were maintained for 40 confinement times and several internal skin times and were only limited by the available pulse length. Continuously reconnecting (1,1) fishbones clamp the current profile in the core and lead to stationary central low shear ( $q_{min} \approx 1$ ). The density in these scenarios was extended up to slightly below half of the Greenwald density to integrate power exhaust and He ash removal by appropriate divertor conditions. With gas fuelling, the threshold heating power for ITB formation had to be raised by  $\approx 50\%$ , where discrimination between a critical value for heat and/or torque input was not yet possible. A density increase caused by improved core particle confinement at more triangular plasma shapes does not change the ITB onset conditions and allows higher  $\beta_N$ -values without destabilizing NTMLs. The more effective impurity screening at higher edge densities reduces  $Z_{eff}$  from 3 (at  $0.35 n_{GW}$ ) to 2 in the plasma centre. No temporal accumulation of impurities is observed, but impurities show centrally peaked densities consistent with neoclassical predictions. First measurements point to sufficient He exhaust in this scenario. In summary, this scenario may offer stationary, inductively driven H-mode operation for ITER with enhanced performance allowing access to ignition even in the ITER FEAT device. A further performance extension may be feasible with the stabilization of the limiting NTM's by ECCD feedback in the island O-points as demonstrated in ELMy H-mode discharges on ASDEX Upgrade [17].

The reversed-shear scenarios ( $q_{min} \approx 2$ ) with internal barriers and L-mode edge were achieved transiently during the current ramp in limiter configuration and quasi-stationary for some confinement times in SN divertor configuration. These discharges show strong pressure gradients with bootstrap currents exceeding 55% of the plasma current. These discharge conditions may therefore offer the route to true steady-state, non-inductively driven tokamak operation combining improved performance and high bootstrap current, but the attainment of steady-state and the MHD limits (including wall stabilization) have to be proved.

Again, the core q-profile can be clamped due to reconnection of, respectively,  $m = 3$  and 2 MHD modes during evolution of the hollow q-profile. Here, the acting (2,1) fishbones do not deteriorate confinement.

Two general results should be mentioned here. In all scenarios discussed, we observed simultaneous ITB's for ion and electron energy, particles and momentum within the experimental uncertainties. Secondly, not discussed in the paper, in all discharges leading to the formation of ITB's the position of the barrier foot remains just at the  $q_{min}$ -radius (see Fig. 4), but no clear correlation of the ITB formation with a rational value of  $q_{min}$  was observed.

Active control by external current drive is required for steady-state operation with low or reversed shear profiles. First experiments on ASDEX Upgrade using simultaneous strong central ion (NBI heating) and electron heating with ECRF in ITB limiter discharges definitely showed ITB's for both electrons and ions simultaneously, without detrimental effects on the reduced ion transport. In particular, with on-axis counter-ECCD it was possible to achieve  $T_e \geq T_i$  operation.

To meet all the requirements for steady-state advanced operation, several technical enhancements are being installed. For high- $\delta$  plasma shapes an adaptation of the divertor for the higher triangular shapes is envisaged for 2000/1. In parallel, the provision for off-axis CD will be extended to sustain and control low/reversed-shear profiles and stabilize MHD modes. This will be achieved in a flexible way by supplementing the existing ECCD (150 kA on-axis/1.6 MW ECRF) by on-axis fast wave ICCD (first experiments in 2000 with up to 150 kA/6 MW ICRF) and off-axis current drive up to 400 kA using more tangential NBI (available in 2001) and ICRF mode conversion. Stationary discharges with reversed shear and  $q_{min} > 2$  should then be possible at a plasma current of 1 MA. Additionally, a flat-top time of 10 s will be available in 2001 by fully exploiting the installed power supplies to get steady-state at  $T_e > 10$  keV not only on the MHD and transport time scales but also on the skin time.

## References

- [1] Levinton F.M. *et al.*, Phys. Rev. Lett. **75**, 4417 (1995).
- [2] Rice B.W. *et al.*, Phys. Plasmas **3**, 1983 (1996).
- [3] Fujita T. *et al.*, Phys. Rev. Lett. **78**, 2377 (1997).
- [4] Soeldner F.X. *et al.*, Nucl. Fusion **39**, 407 (1999).
- [5] Gruber O. *et al.*, Phys. Rev. Lett. **83**, 1787 (1999).

- [6] Gruber O. *et al.*, IAEA-F1-CN-69/OV4/3, Nucl. Fus. 39/Yokohama Special Issue **1**, 1321 (1999).
- [7] Wolf R. *et al.*, Pl. Phys. Contr. Fus. **41**, B93 (1999).
- [8] Guenter S. *et al.*, Pl. Phys. Contr. Fus. **41**, B231 (1999).
- [9] Guenter S. *et al.*, submitted to Nucl. Fus.
- [10] Pereverzev G. *et al.*, 26th EPS (Maastricht) ECA Vol. **23J**, 1429 (1999).
- [11] Stober J. *et al.*, 17th IAEA TCM on H-Mode and Transport Barrier Physics, Pl. Phys. Contr. Fusion.
- [12] Dux R. *et al.*, 26th EPS (Maastricht) ECA Vol. **23J**, 1409 (1999).
- [13] Bosch H.-S. *et al.*, Journ. Nucl. Mat. 266-269 (1999) 462-466.
- [14] Guenter S. *et al.*, accepted by Phys. Rev. Let. Wolf R. *et al.*, accepted by Phys. of Plasmas.
- [15] Pereverzev G. *et al.*, 25<sup>th</sup> EPS (Prague) ECA Vol.22C, 496 (1998).
- [16] Staebler A. *et al.*, 25<sup>th</sup> EPS (Prague) ECA Vol. 22C, 1312 (1998).
- [17] Zohm H. *et al.*, Nucl. Fus. **39**, 577 (1999).